The spectral scalings of magnetic fluctuations upstream and downstream of the Venusian bow shock

S. D. XIAO
Harbin Institute of Technology, Shenzhen
M. Y. Wu
Harbin Institute of Technology Shenzhen
G. Q. Wang
Harbin Institute of Technology Shenzhen
Y. Q. Chen
University of Science and Technology of China
T. L. Zhang (Tielong.Zhang@oeaw.ac.at)
Harbin Institute of Technology; Austrian Academy of Sciences

Express Letter

Keywords: Magnetic fluctuations, Turbulence, Venusian bow shock, Spectral scalings, Shock geometry, Venus Express

Posted Date: December 31st, 2020

DOI: https://doi.org/10.21203/rs.3.rs-27524/v3

Version of Record: A version of this preprint was published on January 7th, 2021. See the published version at https://doi.org/10.1186/s40623-020-01343-7.

The spectral scalings of magnetic fluctuations upstream and downstream of the Venusian bow shock

S. D. Xiao[1], M. Y. Wu[1], G. Q. Wang[1], Y. Q. Chen[2], T. L. Zhang[1,3,*]

[1]Harbin Institute of Technology, Shenzhen, China

[2]CAS Key Laboratory of Geospace Environment, University of Science and Technology of China, Hefei, China

[3]Space Research Institute, Austrian Academy of Sciences, Graz, Austria

Corresponding author: T. L. Zhang (Tielong.Zhang@oeaw.ac.at)

Abstract

We statistically investigate the spectral scalings of magnetic fluctuations at the upstream and downstream regions near the Venusian bow shock and perform a differentiation by shock geometry. Based on the Venus Express data, 115 quasi-parallel ($Q_{\parallel}$) bow shock crossings and 303 quasi-perpendicular ($Q_{\perp}$) bow shock crossings are selected. The statistical results suggest that the bow shock tends to modify the upstream spectra flatter to 1/f noise in the magnetohydrodynamics (MHD) regime and steeper to turbulence in the kinetic regime after the magnetic fluctuations crossing the bow shock, and this modification for the $Q_{\parallel}$ and $Q_{\perp}$ bow shock is basically consistent. While the upstream spectral scalings are associated with the shock geometry. The changes of the spectral scalings of magnetic fluctuations near the $Q_{\parallel}$ bow shocks are not as significant as near the $Q_{\perp}$ bow shock crossings. That might result from the fluctuations generated by the backstreaming ions which can escape across the $Q_{\parallel}$ bow shock into the foreshock. Our results suggest that the energy cascade and dissipation near Venus can be modified by the Venusian bow shock, and the $Q_{\parallel}$ bow shock plays an important role on the energy injection and dissipation in the solar wind interaction with Venus. The large dispersion of spectral scalings indicates that this fluctuation environment is complicated, and the shock geometry is not the only key factor in the fluctuations across the Venusian bow shock. Other possible factors in the shock modification to the upstream fluctuations will be explored in future.

Keywords: Magnetic fluctuations, Turbulence, Venusian bow shock, Spectral scalings, Shock geometry, Venus Express

1. Introduction

As a typical unmagnetized planet, Venus has no global intrinsic magnetic field. An induced magnetosphere is created by the solar wind (SW) interaction with Venus (e.g., Zhang et al., 2008a), consisting of the magnetic barrier (e.g., Zhang et al., 1991, 2008b; Xiao and Zhang, 2018) and the magnetotail (e.g., Rong et al., 2014; Xiao et al., 2016). The Venusian induced magnetosphere can deflect the upstream SW, and a bow shock and a magnetosheath are formed above (e.g., Zhang et al. 2008c, Phillips and McComas, 1991). The near-Venusian space environment is a natural laboratory to investigate the SW interaction with unmagnetized planetary bodies (e.g., Luhmann, 1986). In the near-Venusian space, magnetic field fluctuations play an important role in the transformation of momentum and energy, and their properties are widely reported (e.g., Luhmann et al., 1983; Guicking et al., 2010; Du et al., 2010; Xiao et al., 2017). The power of these fluctuations generally exhibits a frequency function as $P \propto 1/f^{\alpha}$ (where P is the power spectral density (PSD), f is the frequency, and α is the spectral scaling index). The index α is considered as an indicator of the nature of fluctuations, and it generally has different values for the frequency ranges above and below the local proton gyrofrequency ($f_p = eq/m_p$). In the magnetohydrodynamics (MHD) frequency range, the Kolmogorov scaling value of $\alpha \sim 5/3$ is expected for turbulence. Energy cascade occurs in this regime, where the energy is transferred from lower to higher frequencies. In the kinetic frequency range, the turbulence has a larger value of $\alpha \sim 2.8$, in which regime the magnetic energy dissipates into plasma or accumulates by exciting some dispersive waves like the whistler. The spectral scaling indices have been extensively

used to analyze the magnetic field fluctuations and turbulence in the solar wind (e.g., Alexandrova et al., 2008, 2009; Kiyani et al., 2009; Bruno and Carbone, 2013), in the planetary space environments near Earth (e.g., Vörös et al., 2004; 2007; 2011), Mars (e.g., Ruhunusiri et al., 2017), and Venus (e.g., Vörös et al., 2008a, 2008b; Dwivedi et al., 2015; Xiao et al., 2018, 2020a, 2020b).

Although Venus has a similar size to Earth, the Venusian bow shock and magnetosheath are much smaller, with a scale ratio of ~1/10 (e.g., Slavin et al., 1979). This might result in some differences between their space plasma environments. Vörös et al. (2008a, 2008b) reported a survey of the spectral scalings of magnetic fluctuations in the Venusian magnetosheath and wake. They observed 1/f noise in the dayside magnetosheath, wavy structures near the terminator, and MHD turbulence at the magnetosheath post terminator boundary layer and near the nightside bow shock. The observed 1/f noise in the Venusian magnetosheath may indicate that the energy cascade between different scales is absent and the fluctuations are controlled by multiple uncorrelated driving sources (e.g., Vörös et al., 2007). Xiao et al. (2018) further examined the magnetic fluctuations in the dayside Venusian magnetosheath and found a clear difference of the turbulence distributions between downstream of the quasi-parallel ($Q_{\parallel}$) and the quasi-perpendicular ($Q_{\perp}$) shocks. It is speculated that turbulence can be rapidly developed along the streamlines or penetrate into the Venusian magnetosheath downstream of the $Q_{\parallel}$ bow shock. It suggests that the shock geometry has an effect on the spectral scalings of downstream magnetic fluctuations, and the bow shock plays a role on the turbulence distribution in the near-Venusian space. Xiao et al.

(2020a) presented a description of the spectral scalings of magnetic fluctuations at the Venusian bow shock crossings. In terms of the spectral scalings, the dayside-nightside shock crossings exhibit a clear asymmetry. Noisy fluctuations dominate at the dayside shock crossing, and more MHD turbulence is present at the nightside shocks. Moreover, this distribution at the bow shock seems independent on the shock geometry. However, we still rarely know how the bow shock modifies the upstream magnetic fluctuations and turbulence from the SW.

Besides, previous investigations of turbulence near Venus are mainly focused on the MHD regime. It is believed that the spectral scalings of magnetic field fluctuations in the kinetic regime are quite different from those in the MHD regime. A recent research presented the global spatial distribution of the spectral scaling indices of magnetic fluctuations in both of MHD and kinetic regimes, and the global distribution suggests that the kinetic effects on magnetic energy dissipation are common in the near-Venusian space (Xiao et al., 2020b). The SW turbulence can be modified by the Venusian bow shock in both MHD and kinetic regime, and kinetic turbulence extensively occurs in the Venusian magnetosheath and the induced magnetosphere. It is believed that kinetic turbulence plays a prominent role in magnetic energy dissipation and particle heating in such an environment.

In this paper, we aim to the differentiation of the spectral scalings of the magnetic field fluctuations upstream and downstream of the Venusian bow shock and the shock geometry effects. The spectral scaling indices will be examined in both MHD and

kinetic regimes. The investigation of the Venusian bow shock modifications to the upstream SW turbulence can help us to better understand the energy injection, cascade, and dissipation in the SW interaction with Venus.

2. Data and Methods

Venus Express (Svedhem et al., 2007; Titov et al., 2006), as the first ESA's Venus exploration mission, was launched in November 2005 and arrived at Venus in April 2006. Venus Express provides a great opportunity to examine the spectral scalings of the magnetic fluctuations near the Venusian bow shock. In this study, the magnetic field data measured by Venus Express magnetometer (Zhang et al., 2006) at a sampling rate of 32 Hz are used, and the bow shock crossings can be identified by the sudden change in the magnitude of the magnetic field between the SW and the Venusian magnetosheath, as shown in Figure 1a.

Figure 1a shows the total magnetic field time series containing a bow shock crossing on Dec. 30, 2006. To examine the spectral scalings of the upstream and downstream magnetic fluctuations near the Venusian bow shock, the upstream and downstream intervals need to be selected during this shock crossing event. For this inbound case, a 256-s upstream interval is selected before the shock, and a 128-s downstream interval is selected after the shock crossing, as indicated in Figure 1b. Figure 1b shows the magnetic field observations near the bow shock crossing in the aberrated Venus solar

orbital (VSO) coordinate system, where the X axis points antiparallel to the average SW flow (with an aberration angle of 5°) from Venus, the Z axis is perpendicular to the ecliptic plane and toward north, and the Y axis completes the right-handed Cartesian coordinate system. Based on these two intervals, the PSDs are calculated via wavelet transforms (Torrence and Compo, 1998):

$$PSD(f) = \frac{2\Delta t}{N}\sum_{j=1}^{N}\left[W_x^2(t_j, f) + W_y^2(t_j, f) + W_z^2(t_j, f)\right],$$

where Δt is the sampling time, N is the length of the time series, and W_x, W_y, and W_z are the wavelet transforms of the x, y, and z components of the magnetic field.

The upstream and downstream PSDs are respectively shown in Figure 1c and d with dashed f_p. An obvious spectral break near the f_p is present in the downstream PSD, while it is not so clear for the upstream. The spectral break between the MHD and kinetic regimes is generally around f_p. However, the spectral break is not always precisely at f_p. For example, the spectral break may correlate better with the ion plasma frequency under some conditions (Chen et al., 2014). Due to the lack of ion data, here we can distinguish these two regimes using f_p and ignore the transition range around f_p to eliminate the interference. In this study, we refer to the frequency range below $f_p/2$ as the MHD regime and the frequency range above $2f_p$ as the kinetic regime. The value of f_p is typically exhibited as 0.1 Hz in the upstream SW near Venus and 0.3 Hz in the downstream Venusian magnetosheath. The upstream interval is selected longer to cover a lower frequency range. Then the spectral indices in the MHD regime (α_m) and the kinetic regime (α_k) can be estimated as the slopes of the power-frequency

log-log plot of the corresponding PSD in the frequency ranges of concern. Based on the methods described above, a statistical study of the spectral indices is performed at the upstream and downstream regions near the Venusian bow shock in the next section.

3. Statistical Observations

To statistically differentiate the spectral scaling indices for the upstream and downstream regions near the Venusian bow shock and emphasize the shock geometry effects, we examine the Venus Express magnetic field data for ~7 years (2006.05~2012.08) and identify the bow shock crossings. Firstly, we select the orbits when the interplanetary magnetic field (IMF) is relatively steady; that is, the directional changes of the IMF between inbound and outbound crossings of bow shock (~15-min time interval) are less than 30°. Secondly, the shape of the Venusian bow shock can be estimated based on the positions of these two bow shock crossings and the conic section equation $R = L/(1 + e\cos\theta)$ with a focus at (x_0, 0, 0) and a fixed e of 1.03 during solar minimum (2006-2010) or 1.095 during solar maximum (2011-2012) as reported by Shan et al. (2015), where R is the bow shock distance from the conic focus, L is the conic section semi-latus rectum, and e is the eccentricity. At last, we find 209 orbits/418 shock crossings with steady IMF and well-determined bow shock model.

We calculate the PSDs of the upstream and downstream intervals of these shock crossings, and then the values of α_m and α_k can be estimated in the corresponding

frequency ranges, with the method described above. Figure 2 shows the histograms of α for the upstream and the downstream intervals of the 418 shock crossings in the MHD and kinetic regimes. We find that, as shown in Figures 2a and 2b, the median values of α_m are 1.26 and 1.03 and the mean values are 1.25 and 1.09 with the standard deviations of 1.07 and 1.10 for the upstream and the downstream intervals, respectively. The statistical distributions indicate that these magnetic fluctuations are in a developing and mixed state. From upstream to downstream, the values of α_m show a decreasing trend and the downstream fluctuations tend towards 1/f noise in the MHD regime. This can be ascribed to the fact that collisionless shock physics is mediated by particles and that the injection scale tends to be close to the proton kinetic scale. Since the analysis is performed close to the bow shock, the turbulence has not fully developed yet. Similar features can also be observed downstream of the Earth bow shock (e.g., Yordanova et al., 2008). Figures 2c and 2d indicate the median values of α_k are 2.27 and 2.88 and the mean values are 2.26 and 2.80 with the standard deviations of 0.72 and 0.54 for the upstream and the downstream intervals, respectively. The values of α_k for the downstream tend to be larger and concentrated, and the downstream distribution indicates that the kinetic turbulence dominates behind the bow shock. As reported by a previous study (Xiao et al., 2020b), well developed turbulence is a common phenomenon in the pristine SW near Venus. However, Figure 2 shows that although some spectral indices indicating the turbulence can still be found, these upstream intervals are rarely turbulence dominant. We infer that the SW fluctuations have been modified before they reach the bow shock.

To be noticed, we can find that the histograms in Figure 2 exhibit large dispersions. That indicates the complex and diverse magnetic fluctuations near the Venusian bow shock, and the spectral scalings of the fluctuations could be affected by multiple factors. Some previous studies suggested that the bow shock geometry could affect the fluctuations and turbulence in the near-Venusian space (e.g., Luhmann et al., 1983; Xiao et al., 2018). To further investigate the bow shock modifications to the SW fluctuations and turbulence, we split the bow shock crossings into two categories of $Q_{\parallel}$ ($\theta_{BN} < 45°$) and $Q_{\perp}$ ($\theta_{BN} > 45°$) geometries. The shock normal angle θ_{BN} can be calculated by the average upstream magnetic field and the estimated local bow shock normal. The average upstream magnetic field is obtained in the 256-s upstream interval of each shock crossing event. The shock normal is determined by the estimated bow shock model with the method described above. Consequently, 115 $Q_{\parallel}$ events and 303 $Q_{\perp}$ events are obtained, and then we can examine the shock geometry effects on the spectral scalings of fluctuations near the bow shock. Here we show two examples of the magnetic field observations in Figure 3 for the $Q_{\parallel}$ and the $Q_{\perp}$ bow shock crossings. Figures 3a and 3b present the total magnetic field, and Figures 3c and 3d present the magnetic fields in the aberrated VSO coordinate system. Figures 3a and 3c present a $Q_{\parallel}$ bow shock (θ_{BN}~28.4°) crossing event on May 16, 2006. Figures 3b and 3d present a $Q_{\perp}$ bow shock (θ_{BN}~84.0°) crossing event on Nov. 18, 2006. This indicates the high level of excited fluctuations upstream of the $Q_{\parallel}$ shock by backstreaming ions in comparison with the $Q_{\perp}$ configuration.

Figure 4 shows the histograms of α for the upstream and the downstream intervals of

206 the $Q_{\parallel}$ (red) and $Q_{\perp}$ (blue) bow shock crossings. Figures 4a and 4b show the
207 histograms of α_m. The median values of α_m for the downstream intervals of $Q_{\parallel}$ and
208 $Q_{\perp}$ bow shocks are 0.96 and 1.05, respectively. The similar distributions suggest that,
209 in the MHD regime, the effects of the bow shock on the SW fluctuations and turbulence
210 are independent on the shock geometry. While the values of α_m for the upstream
211 intervals are obviously related to the shock geometry. For the upstream intervals of $Q_{\parallel}$
212 and $Q_{\perp}$ bow shocks, the median values of α_m are 0.82 and 1.43, respectively. Both
213 distributions upstream and downstream of the $Q_{\parallel}$ bow shocks present two peaks at ~1
214 and ~1.5. The spectral scalings do not show significant differences between the
215 fluctuations upstream and downstream of the $Q_{\parallel}$ shocks. The MHD fluctuations
216 upstream of the $Q_{\perp}$ bow shocks are also in a mixed state that some fluctuations might
217 be modified or still in developing, but the distribution is more like the SW with pre-
218 existing turbulence. Obvious differences exist between the upstream and downstream
219 intervals of the $Q_{\perp}$ shocks, which could result from the waves excited behind the $Q_{\perp}$
220 shocks. We infer that the pre-existing MHD turbulence from the SW could be more
221 prone to reaching the $Q_{\perp}$ bow shocks but start to be modified before reaching the $Q_{\parallel}$
222 bow shocks. The modification might be due to the waves generated near the bow shock.

223 Figures 4c and 4d show the histograms of α_k. The median values of α_k are 2.88 and
224 2.87 for the downstream intervals of $Q_{\parallel}$ and $Q_{\perp}$ bow shocks, respectively. The
225 distributions indicate that the kinetic turbulence is significantly dominant for the
226 downstream intervals, and it is not shock geometry dependent. The upstream kinetic
227 fluctuations also show a difference between the $Q_{\parallel}$ and $Q_{\perp}$ bow shock crossings. The

median values of α_k for the upstream intervals of $Q_{\parallel}$ and $Q_{\perp}$ bow shocks are respectively 2.70 and 2.11. The statistical kinetic spectral scalings of the fluctuations near the $Q_{\parallel}$ bow shocks do not change significantly as near the $Q_{\perp}$ bow shocks, but the values of α_k for the downstream intervals have a much more concentrated distribution. This indicates that the downstream kinetic turbulence is mainly developed behind the bow shock but not penetrate from the upstream. The kinetic turbulence can also be developed upstream of the $Q_{\parallel}$ bow shocks. We infer that the SW kinetic fluctuations could be affected by the Venusian bow shock at the upstream region and the upstream difference of the $Q_{\parallel}$ and $Q_{\perp}$ bow shock might result from the more backstreaming ions upstream of the $Q_{\parallel}$ bow shock.

Based on the results from Figure 4, we find the shock geometry does influence the spectral scalings of magnetic fluctuations upstream and downstream of the Venusian bow shock. However, a large dispersion is still shown in some histograms. Therefore, the shock geometry is one key factor but not the only factor in the propagation of the fluctuations across the Venusian bow shock.

4. Discussion and Conclusions

In this paper, we use the magnetic field data of Venus Express from 2006.05 to 2012.08 to investigate the spectral scalings variations of the magnetic field fluctuations near the Venusian bow shock. The spectral indices are calculated in the MHD and kinetic

248 regimes for the upstream and downstream intervals close to the Venusian bow shock.
249 There are 115 $Q_{\parallel}$ and 303 $Q_{\perp}$ shock crossings selected in this study. Based on the
250 statistical results, the shock effects on the spectral scalings near the Venusian bow
251 shocks are examined.

252 We find the Venusian bow shock tends to flatten the spectra of upstream MHD
253 fluctuations and steepen the kinetic spectra. At the downstream regions, the MHD
254 magnetic fluctuations and turbulence tend to be modified to 1/f noise and the kinetic
255 turbulence can be fully developed behind the shock, which is consistent with the
256 previous studies (e.g., Vörös et al., 2008a; Xiao et al., 2020b). This suggests that the
257 energy cascade and dissipation near Venus can be modified by the Venusian bow shock.
258 The spectral indices for the downstream intervals show this shock modification is
259 independent on the shock geometry. However, we find the upstream spectral scalings
260 are associated with the shock geometry. In the MHD regime, the spectra upstream of
261 $Q_{\parallel}$ bow shocks are flatter than of $Q_{\perp}$ bow shocks. In the kinetic regime, the spectra
262 upstream of $Q_{\parallel}$ bow shocks are steeper than of $Q_{\perp}$ bow shocks. As reported by a
263 previous study, the α_m in the pristine solar wind far upstream of the Venusian bow
264 shock is near Kolmogorov scaling value and the values of α_k are typically ~2.5-3
265 (Xiao et al., 2020b). Our results in this study indicate that the bow shock effects on the
266 SW fluctuations could begin at the upstream region, which might result from reflected
267 ions and newborn pickup ions. Such as, the ULF waves excited by backstreaming ions
268 exhibit their frequency range of 0.3-0.5f_p (e.g., Shan et al., 2016), which could lead to
269 a decrease of α_m, and the whistler-mode waves generated upstream of the bow shock

exhibit their frequency range from several f_p to 2 Hz (e.g., Russell, 2007), which could lead to an increase of α_k. For validating the PSDs in the spacecraft frame, the possibility of violation the Taylor hypothesis need to be considered, especially at high frequencies and in an environment close to a shock (e.g., Klein et al., 2014). Unfortunately, because of the limited observational data, it is hard to detect the violation of the Taylor hypothesis in this study. Multiple wave modes can be generated near the bow shock, and sometimes the spectral shape might be not clear for the fluctuations in the shock-upstream and shock-downstream regions. The values of α in this region exhibit a large variation. To interpret these fluctuations, we further examine their compression and rotation senses (Arthur et al., 1976; Means, 1972), as with some prior studies on magnetic field fluctuations near Venus (e.g., Guicking et al., 2010; Du et al., 2010; Xiao et al., 2017). The histograms of these fluctuation properties are shown in Figure 5 for the $Q_{\parallel}$ (red) and $Q_{\perp}$ (blue) events.

The transverse and compressional ratio (ζ) of fluctuations is defined as $(P_{\perp} - P_{\parallel})/P_T$, where $P_{\perp}$ is the transverse power of the fluctuations with respect to the ambient magnetic field, $P_{\parallel}$ is the compressional power, and P_T is the total power. The range of ζ is from -1 to 1. A positive (negative) ratio means the transverse power is higher (lower) than the compressional power, and a ratio of 1 indicates that this fluctuation is purely transverse. Figures 5a-5d show the histograms of ζ in the MHD and kinetic regimes. In the MHD regime, we can find the upstream fluctuations are mainly transverse, while more compressional fluctuations are present downstream, especially behind the $Q_{\perp}$ bow shock. That might be due to the compressional waves generated

by the mirror mode instability (e.g., Volwerk et al., 2008). In the kinetic regime, the transverse fluctuations dominate in the region near the Venusian bow shock, and this nature is shock geometry independent.

The ellipticity (ε) of fluctuations is defined as the ratio of the minor to major axis of the polarization ellipse transcribed by the field variations of the components transverse to the ambient field (Samson and Olson, 1980). The sign indicates the direction of rotation of the polarization ellipse, i.e., the rotation sense about the ambient field (Means, 1972). Negative signs refer to left-handed polarized waves and positive signs refer to right-handed polarized waves. The waves of linear and circular polarization correspond to the ε of 0 and ±1, respectively. Figures 5e-5h show the histograms of ε in the MHD and kinetic regimes. The histograms indicate that many right-handed polarized fluctuations can be generated behind the bow shock, and they could be excited by the pickup ions. In addition, we consider that these left-handed polarized waves in kinetic regime, which are hardly observed downstream, are related to the upstream whistler-mode waves or so-called 1-Hz waves generated at the bow shock and propagating upstream (e.g., Russell, 2007; Xiao et al., 2020). These waves are elliptically polarized and intrinsically right-handed polarized; however, they are observed left-handed elliptically polarized in spacecraft frame due to the Doppler shifting effect.

At the $Q_{\parallel}$ shocks, some ions can escape into the foreshock region, and a variety of large-amplitude waves can be excited by these backstreaming ions (e.g., Delva et al.

2011, Collinson et al., 2012; Shan et al., 2013). These waves generated in the foreshock can be convected to the downstream side across the $Q_{\parallel}$ bow shock (e.g., Luhmann et al., 1983; Du et al., 2010; Shan et al., 2014). That might be a reason of the statistical finding that there are no significant variations of the spectral scalings of magnetic fluctuations near the $Q_{\parallel}$ bow shocks. This suggests that the $Q_{\parallel}$ bow shock is an important channel of the energy injection and dissipation in the interaction of the SW with Venus. More fluctuations and higher energies are injected at $Q_{\parallel}$ rather than $Q_{\perp}$ shocks. At the $Q_{\perp}$ shocks, these ions will generally gyrate back and then excite waves behind the shocks (e.g., Volwerk et al., 2008). These waves could result in the changes of downstream spectral scalings. However, in some cases, the waves upstream of $Q_{\perp}$ shocks can be transmitted into the downstream, and the downstream spectra could also be similar to the upstream except an enhanced amplitude (e.g., Lu et al., 2009). Thereby, the spectral scalings variations across the bow shock could be controlled by multiple factors. In this study, we find the shock geometry is an important factor. Other possible factors affecting the Venusian bow shock modification to the SW fluctuations will be our future topics.

Declarations

Availability of data and materials

Venus Express magnetic field data are available in the ESA's Planetary Science Archive (ftp://psa.esac.esa.int/pub/mirror/VENUS-EXPRESS/).

Competing interests

The authors declare that they have no competing interests.

Consent for publication

Not applicable.

Funding

This work was supported by NSFC grants (41904156, 41974205, 41774171, 41774167 and 41804157), the project funded by China Postdoctoral Science Foundation (2019M651271), the pre-research Project on Civil Aerospace Technologies (No. D020103) funded by CNSA, Shenzhen Science and Technology Research Program (JCYJ20180306171918617) and Shenzhen Science and Technology Program (Group No. KQTD20180410161218820). Tielong Zhang was supported by CAS Center for Excellence in Comparative Planetology.

Authors' contributions

SDX initiated the investigation and prepared the original manuscript. TLZ supervised the investigation. MYW and GQW participated in the discussions and reviewed the manuscript. YQC and TLZ gave the suggestions of the manuscript. All authors read and approved the final manuscript.

Acknowledgments

The authors are grateful to the supports of NSFC (41904156, 41974205, 41774171, 41774167, 41804157), China Postdoctoral Science Foundation (2019M651271), and the pre-research Project on Civil Aerospace Technologies (No. D020103) funded by CNSA. The authors also acknowledge the financial support of Shenzhen Science and Technology Research Program (JCYJ20180306171918617) and Shenzhen Science and Technology Program (Group No. KQTD20180410161218820), and the support of CAS Center for Excellence in Comparative Planetology.

360 **Reference**

361 Alexandrova, O., Carbone, V., Veltri, P., Sorriso-Valvo, L. (2008). Small-scale energy
362 cascade of the solar wind turbulence. Astrophysical Journal, 674(2), 1153-1157.

363 Alexandrova, O., Saur, J., Lacombe, C., Mangeney, A., Mitchell, J., Schwartz, S. J., et
364 al. (2009). Universality of solar-wind turbulent spectrum from mhd to electron
365 scales. Physical Review Letters, 103(16), 165003.

366 Arthur, C. W., R. L. McPherron, and J. D. Means (1976), A comparative study of three
367 techniques for using the spectral matrix in wave analysis, *Radio Sci.*, 11(10), 833-
368 845, doi:10.1029/RS011i010p00833.

369 Bruno, R., & Carbone, V. (2013). The solar wind as a turbulence laboratory. Living
370 Reviews in Solar Physics, 10(1), 1-208.

371 Chen, C. H. K., Leung, L., Boldyrev, S., Maruca, B. A., Bale, S. D. (2014), Ion-scale
372 spectral break of solar wind turbulence at high and low beta, Geophys. Res. Lett.,
373 41, 8081– 8088, doi:10.1002/2014GL062009.

374 Collinson, G. A., Wilson, L. B., Sibeck, D. G., Shane, N., Zhang, T. L., Moore, T. E.,
375 Coates, A. J., and Barabash, S. (2012), Short large-amplitude magnetic structures
376 (SLAMS) at Venus, J. Geophys. Res., 117, A10221, doi:10.1029/2012JA017838.

377 Delva, M., Mazelle, C., Bertucci, C., Volwerk, M., Vörös, Z., and Zhang, T. L. (2011),
378 Proton cyclotron wave generation mechanisms upstream of Venus, J. Geophys.

Res., 116, A02318, doi:10.1029/2010JA015826.

Du, J., Zhang, T. L., Baumjohann, W., Wang, C., Volwerk, M., Vörös, Z., & Guicking, L. (2010). Statistical study of low-frequency magnetic field fluctuations near Venus under the different interplanetary magnetic field orientations. Journal of Geophysical Research, 115, A12251. https://doi.org/10.1029/2010JA015549

Dwivedi, N. K., Schmid, D., Narita, Y., Kovács, P., Vörös, Z., Delva, M., & Zhang, T. (2015). Statistical investigation on the power-law behavior of magnetic fluctuations in the Venusian magnetosheath. Earth, Planets and Space, 67(1), 137.

Guicking, L., Glassmeier, K. H., Auster, H. U., Delva, M., Motschmann, U., Narita, Y., & Zhang, T. L. (2010). Low-frequency magnetic field fluctuations in Venus' SW interaction region: Venus Express observations. Annales Geophysicae, 28, 951–967.

Kiyani, K. H., Chapman, S. C., Khotyaintsev, Y. V., Dunlop, M. W., & Sahraoui, F. (2009). Global scale-invariant dissipation in collisionless plasma turbulence. Physical Review Letters, 103(7), 075006.

Klein, K., Howes, G., & Tenbarge, J. (2014). The violation of the Taylor hypothesis in measurements of solar wind, turbulence. The Astrophysical Journal Letters, 790(2).

Lu, Q., Hu, Q., & Zank, G P. (2009). The interaction of Alfvén waves with perpendicular shocks. astrophysical journal, 706(1), 687.

Luhmann, J. G., Tatrallyay, M., Russell, C. T., & Winterhalter, D. (1983). Magnetic field fluctuations in the Venus magnetosheath. Geophysical Research Letters, 10(8), 655–658. https://doi.org/10.1029/GL010i008p00655

Luhmann, J.G. (1986). The SW interaction with Venus. Space Sci. Rev. 44, 241–306

Means, J. D. (1972), Use of the three-dimensional covariance matrix in analyzing the polarization properties of plane waves, *J. Geophys. Res.*, 77(28), 5551-5559, doi:10.1029/JA077i028p05551.

Phillips, J.L. and McComas, D.J. (1991). The magnetosheath and magnetotail of Venus. Space Sci Rev 55, 1–80. https://doi.org/10.1007/BF00177135

Rong, Z. J., Barabash, S., Futaana, Y., Stenberg, G., Zhang, T. L., Wan, W. X., Wei, Y., Wang, X.-D., Chai, L. H., and Zhong, J. (2014), Morphology of magnetic field in near-Venus magnetotail: Venus express observations, J. Geophys. Res. Space Physics, 119, 8838– 8847, doi:10.1002/2014JA020461.

Ruhunusiri, S., Halekas, J. S., Espley, J. R., Mazelle, C., Brain, D., Harada, Y., DiBraccio, G. A., Livi, R., Larson, D. E.,... Howes, G. G. (2017). Characterization of turbulence in the Mars plasma environment with MAVEN observations. J. Geophys. Res. Space Phys., 122(1), 656–674. https://doi.org/10.1002/2016JA023456

Russell, C.T., 2007. Upstream whistler-mode waves at planetary bow shocks: a brief review. J. Atmos. Sol. Terr. Phys. 69 (14), 1739–1746

418 Samson, J.C. and Olson, J.V. (1980), Some comments on the descriptions of the
419 polarization states of waves. Geophysical Journal of the Royal Astronomical
420 Society, 61: 115-129. https://doi.org/10.1111/j.1365-246X.1980.tb04308.x

421 Shan, L., Lu, Q., Wu, M., Gao, X., Huang, C., Zhang, T., and Wang, S. (2014),
422 Transmission of large-amplitude ULF waves through a quasi-parallel shock at
423 Venus, J. Geophys. Res. Space Physics, 119, 237– 245,
424 doi:10.1002/2013JA019396.

425 Shan, L., Lu, Q., Mazelle, C., Huang, C., Zhang, T., Wu, M., et al. (2015). The shape
426 of the venusian bow shock at solar minimum and maximum: Revisit based on vex
427 observations. Planetary and Space Science, 109-110(1), 32–37.
428 https://doi.org/10.1016/j.pss.2015.01.004

429 Slavin, J. A., Elphic, R. C., Russell, C. T., Intriligator, D. S., &Wolfe, J. H. (1979).
430 Position and shape ofthe Venus bow shock: Pioneer Venus Orbiter observations.
431 Geophysical Research Letters, 6(11), 901–904.
432 https://doi.org/10.1029/GL006i011p00901

433 Svedhem, H., Titov, D. V., McCoy, D., Lebreton, J. P., Barabash, S., Bertaux, J. L., et
434 al. (2007). The first European mission to Venus. Planetary and Space Science,
435 55(12), 1636–1652. https://doi.org/10.1016/j.pss.2007.01.013

436 Titov, D. V., Svedhem, H., Koschny, D., Hoofs, R., Barabash, S., Bertaux, J. L., et al.
437 (2006). Venus Express science planning. Planetary and Space Science, 54(13-14),

1279–1297. https://doi.org/10.1016/j.pss.2006.04.017

Volwerk, M., Zhang, T. L., Delva, M., Vörös, Z., Baumjohann, W., & Glassmeier, K.-H. (2008). First identification of mirror mode waves in Venus' magnetosheath? Geophysical Research Letters, 35, L12204. https://doi.org/10.1029/2008GL033621

Vörös, Z., Baumjohann, W., Nakamura, R., Volwerk, M., Runov, A., Zhang, T. L., et al. (2004). Magnetic turbulence in the plasma sheet. Journal of Geophysical Research, 109, A11215. https://doi.org/10.1029/2004JA010404

Vörös, Z., Baumjohann, W., Nakamura, R., Runov, A., Volwerk, M., Asano, Y., Jankovičová, D., Lucek, E. A., and Rème, H. (2007). Spectral scaling in the turbulent Earth's plasma sheet revisited, Nonlin. Processes Geophys., 14, 535–541, https://doi.org/10.5194/npg-14-535-2007.

Vörös, Z., Zhang, T. L., Leubner, M. P., Volwerk, M., Delva, M., Baumjohann, W., & Kudela, K. (2008a). Magnetic fluctuations and turbulence in the Venus magnetosheath and wake. Geophysical Research Letters, 35, L11102. https://doi.org/10.1029/2008GL033879

Vörös, Z., Zhang, T. L., Leubner, M. P., Volwerk, M., Delva, M., & Baumjohann, W. (2008b). Intermittent turbulence, noisy fluctuations, and wavy structures in the Venusian magnetosheath and wake. Journal of Geophysical Research, 113, E00B21. https://doi.org/10.1029/2008JE003159

458 Vörös, Z. (2011). Magnetic reconnection associated fluctuations in the deep
459 magnetotail: ARTEMIS results, Nonlin. Processes Geophys., 18, 861–869,
460 https://doi.org/10.5194/npg-18-861-2011.

461 Xiao, S. D., Zhang, T. L., and Wang, G. Q. (2017). Statistical study of low frequency
462 magnetic field fluctuations near Venus during the solar cycle. J. Geophys. Res.
463 Space Phys., 122(8), 8409–8418.

464 Xiao, S. D., Zhang, T. L., & Vörös, Z. (2018). Magnetic fluctuations and turbulence in
465 the Venusian magnetosheath downstream of different types of bow shock. Journal
466 of Geophysical Research: Space Physics, 123, 8219–8226.
467 https://doi.org/10.1029/2018JA025250

468 Xiao, S. D., Zhang, T. L., Vörös, Z., Wu, M. Y., Wang, G. Q., & Chen, Y. Q. (2020a).
469 Turbulence near the Venusian bow shock: Venus Express observations. Journal of
470 Geophysical Research: Space Physics, 125, e2019JA027190.
471 https://doi.org/10.1029/2019JA027190

472 Xiao, S. D., Wu, M. Y., Wang, G. Q., Wang, G., Chen, Y. Q., & Zhang, T. L. (2020b).
473 Turbulence in the near-Venusian space: Venus Express observations. Earth Planet.
474 Phys., 4(1), 82–87.doi: 10.26464/epp2020012

475 Yordanova, E., Vaivads, A., Andre, M., Buchert, S. C., & Voeroes, Z. (2008).
476 Magnetosheath plasma turbulence and its spatiotemporal evolution as observed by
477 the cluster spacecraft. Physical Review Letters, 100(20), 205003.

Zhang, T.L., Luhmann, J.G., Russell, C.T., (1991). The magnetic barrier at Venus. J. Geophys. Res. 96, 11145–11153.

Zhang, T. L., Baumjohann, W., Delva, M., Auster, H.-U., Balogh, A., Russell, C. T., et al. (2006). Magnetic field investigation of the Venus plasma environment: Expected new results from Venus Express. Planetary and Space Science, 54(13–14), 1336–1343. https://doi.org/10.1016/j.pss.2006.04.018

Zhang, T.L., et al., (2008a). Induced magnetosphere and its outer boundary at Venus. J. Geophys. Res. 113, E00B20. https://doi.org/10.1029/2008JE003215.

Zhang, T.L., Delva, M., Baumjohann, W., et al. (2008b). Initial Venus Express magnetic field observations of the magnetic barrier at solar minimum. Planet. Space Sci. 56 (6), 790–795.

Zhang, T. L., et al. (2008c), Initial Venus Express magnetic field observations of the Venus bow shock location at solar minimum, Planet. Space Sci., 56, 785–789, doi:10.1016/j.pss.2007.09.012.

493 **Figure Legends**

494 **Figure 1.** A Venusian bow shock crossing event observed by Venus Express on 30 Dec.
495 2006. Panel a presents the time series of the total magnetic field and the shock crossing
496 interval is shown in shadow. Panel b presents the magnetic field observations near the
497 bow shock in the aberrated VSO coordinate system, and the upstream and downstream
498 intervals are indicated. Panels c and d present the PSDs of the magnetic fluctuations for
499 the upstream and downstream intervals.

500 **Figure 2.** Histograms of the spectral indices for (a, c) the upstream and (b, d) the
501 downstream intervals of the bow shock crossings. The upper panels a and b show the
502 histograms for the MHD regime, and the lower panels c and d show the histograms for
503 the kinetic regime.

504 **Figure 3.** The time series of the magnetic field magnitude and components for the two
505 types of shock geometry encountered during the Venusian bow shock crossings. The
506 left panels a and c present the magnetic field observations near a $Q_{\parallel}$ bow shock on
507 2006 May 16. The right panels b and d present the magnetic field observations near a
508 $Q_{\perp}$ bow shock on 2006 November 18.

509 **Figure 4.** Histograms of the spectral indices for (a, c) the upstream and (b, d) the
510 downstream intervals of the $Q_{\parallel}$ (red) and $Q_{\perp}$ (blue) bow shock crossings. The upper
511 panels a and b show the histograms for the MHD regime, and the lower panels c and d
512 show the histograms for the kinetic regime.

513 **Figure 5.** Histograms of (a-d) the transverse and compressional ratio and (e-h) the
514 ellipticity of fluctuations for the upstream and the downstream intervals of the $Q_{\parallel}$ (red)
515 and $Q_{\perp}$ (blue) bow shock crossings. The upper panels show the histograms for the
516 MHD regime, and the lower panels show the histograms for the kinetic regime.

517

Figures

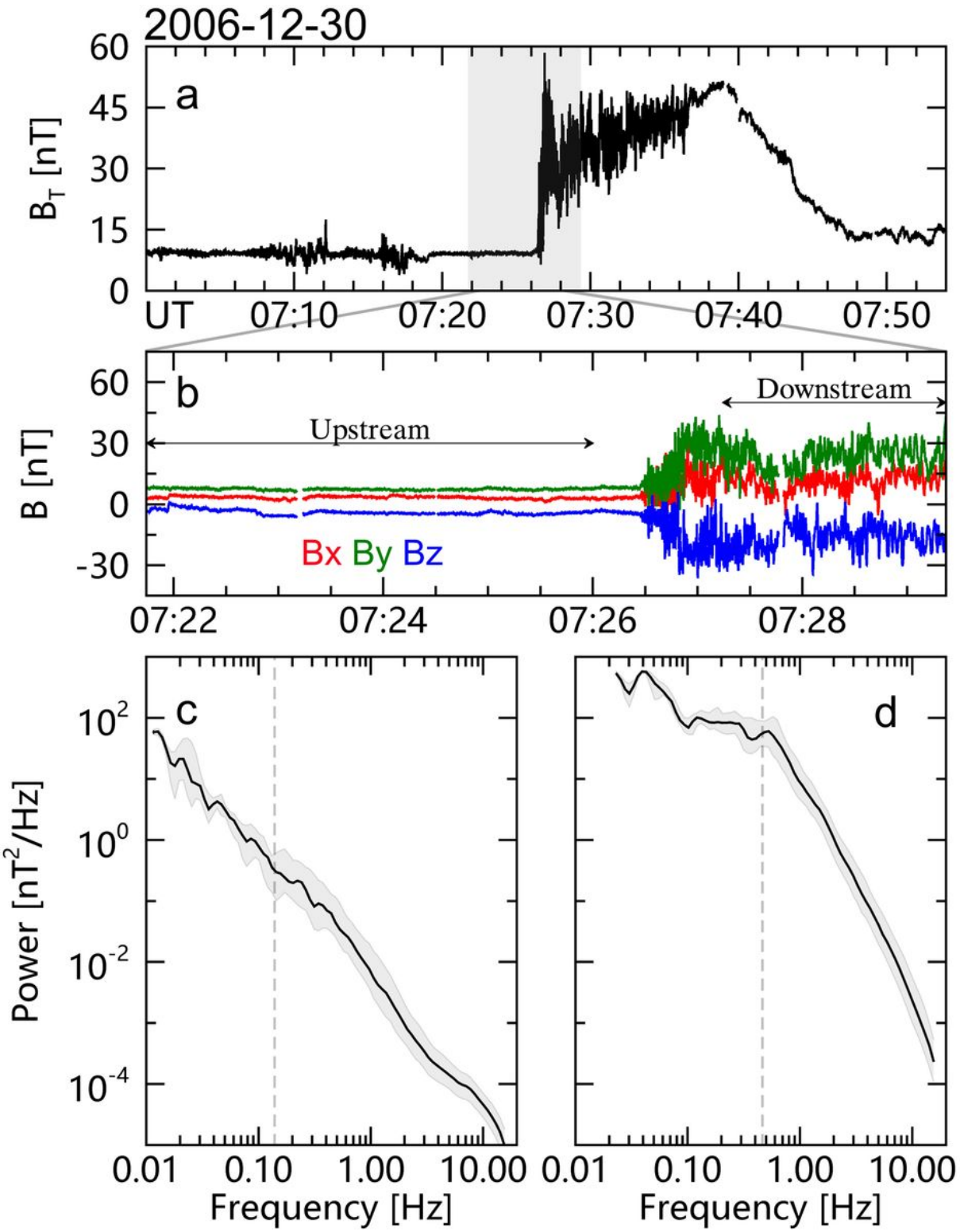

Figure 1

A Venusian bow shock crossing event observed by Venus Express on 30 Dec. 2006. Panel a presents the time series of the total magnetic field and the shock crossing interval is shown in shadow. Panel b presents the magnetic field observations near the bow shock in the aberrated VSO coordinate system,

and the upstream and downstream intervals are indicated. Panels c and d present the PSDs of the magnetic fluctuations for the upstream and downstream intervals.

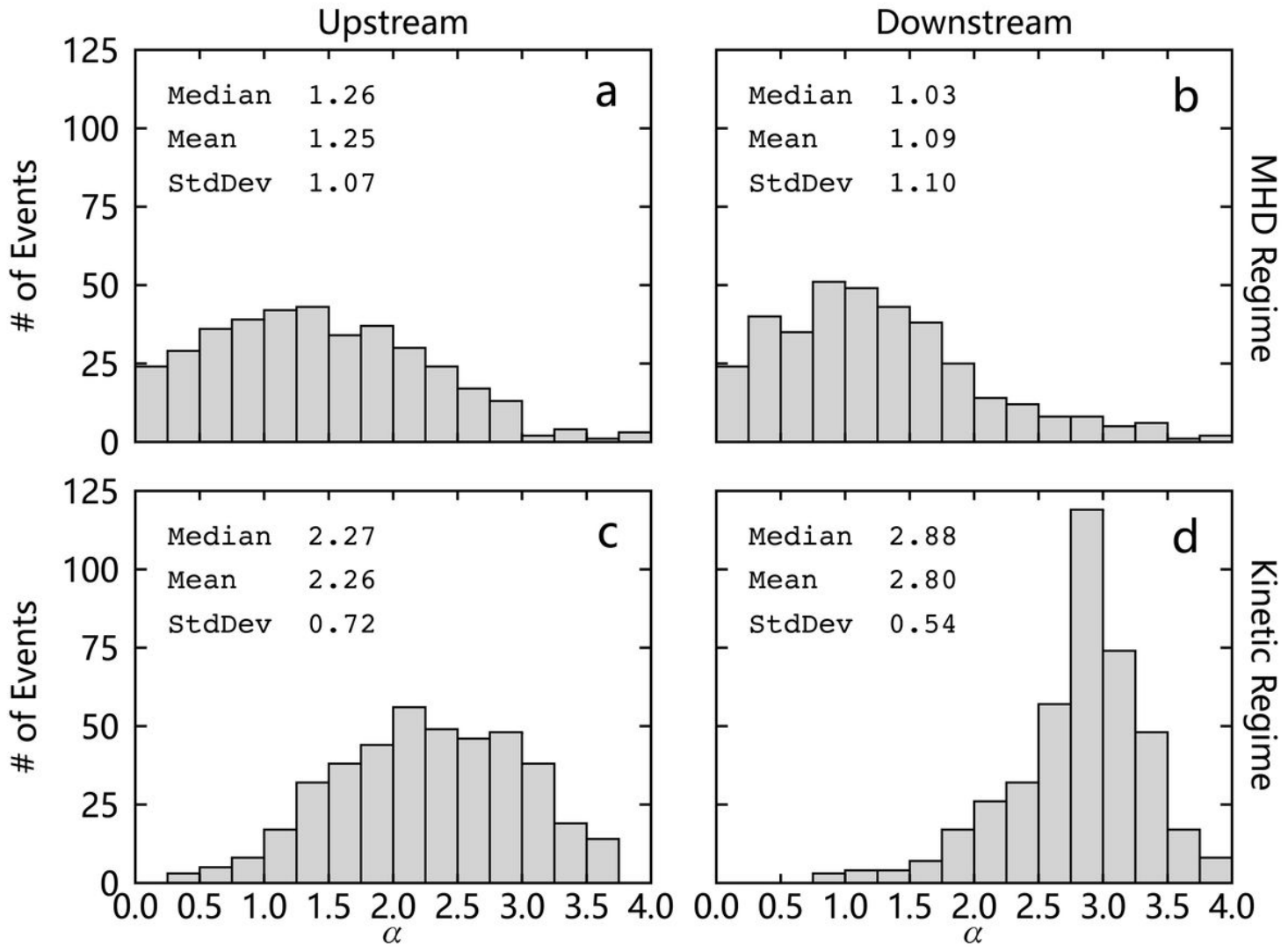

Figure 2

Histograms of the spectral indices for (a, c) the upstream and (b, d) the downstream intervals of the bow shock crossings. The upper panels a and b show the histograms for the MHD regime, and the lower panels c and d show the histograms for the kinetic regime.

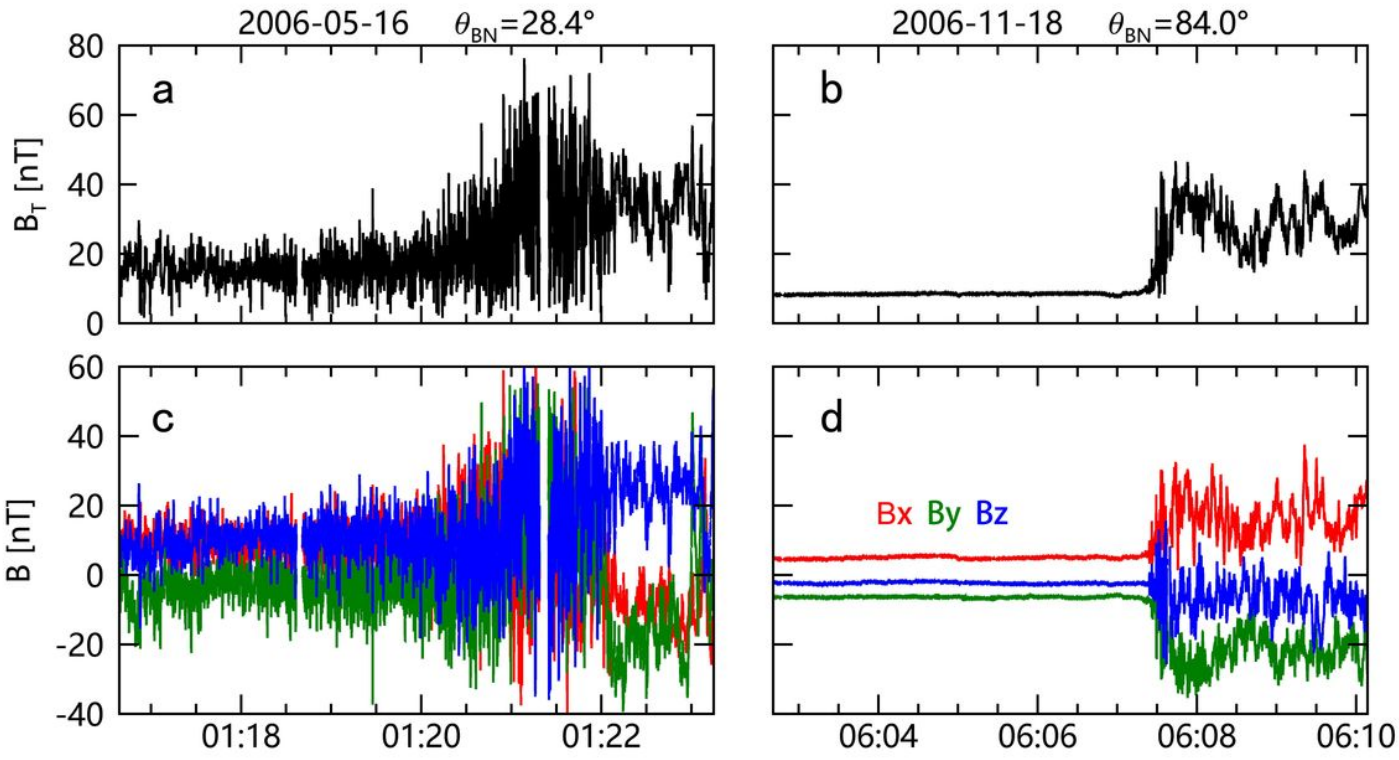

Figure 3

The time series of the magnetic field magnitude and components for the two types of shock geometry encountered during the Venusian bow shock crossings. The left panels a and c present the magnetic field observations near a Q_ bow shock on 2006 May 16. The right panels b and d present the magnetic field observations near a Q_ bow shock on 2006 November 18.

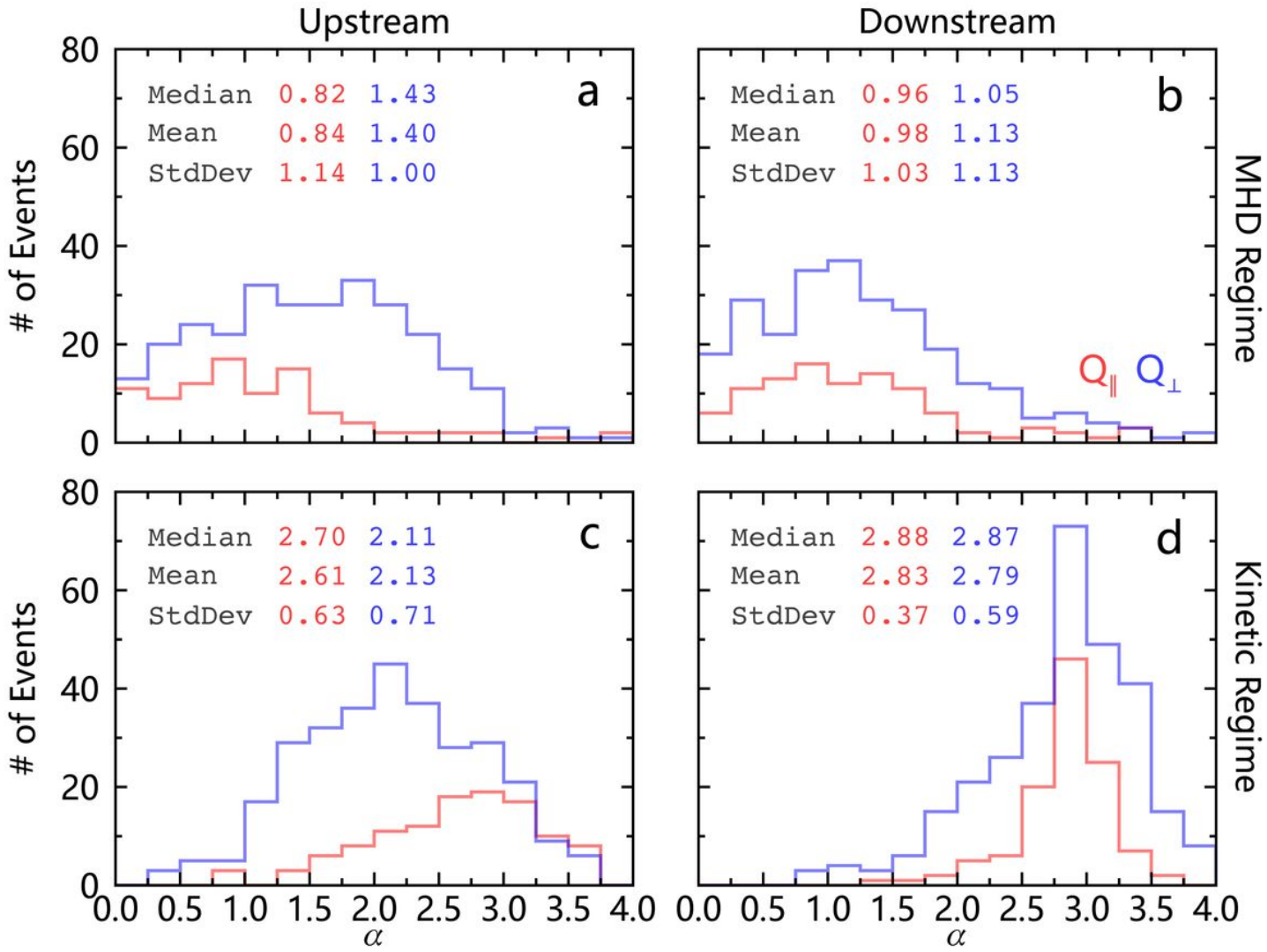

Figure 4

Histograms of the spectral indices for (a, c) the upstream and (b, d) the downstream intervals of the Q_∥ (red) and Q_⊥ (blue) bow shock crossings. The upper panels a and b show the histograms for the MHD regime, and the lower panels c and d show the histograms for the kinetic regime.

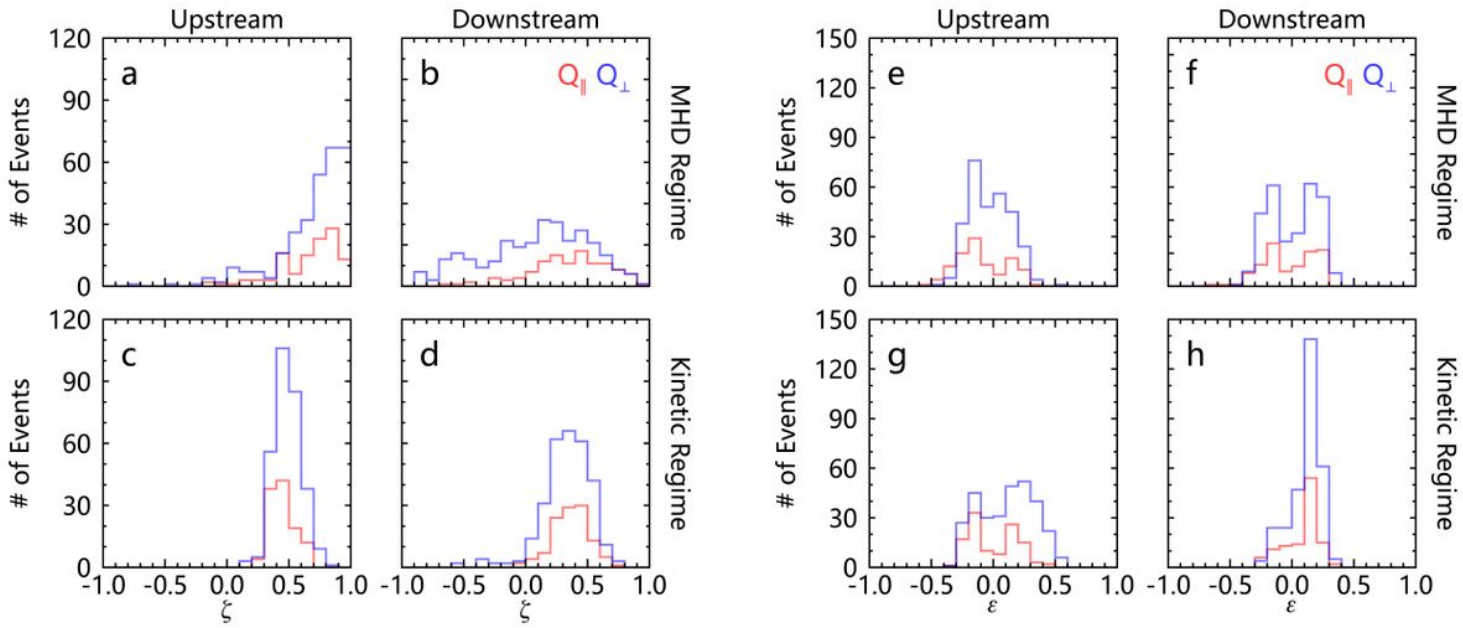

Figure 5

Histograms of (a-d) the transverse and compressional ratio and (e-h) the ellipticity of fluctuations for the upstream and the downstream intervals of the Q_⊥ (red) and Q_∥ (blue) bow shock crossings. The upper panels show the histograms for the MHD regime, and the lower panels show the histograms for the kinetic regime.

Supplementary Files

This is a list of supplementary files associated with this preprint. Click to download.

- AbstractFigure.jpg